PROCEEDINGS OF SPIE

SPIEDigitalLibrary.org/conference-proceedings-of-spie

Quantitative determination of maximal imaging depth in all-NIR multiphoton microscopy images of thick tissues

Pinaki Sarder, Walter Akers, Gail Sudlow, Siavash Yazdanfar, Samuel Achilefu

Pinaki Sarder, Walter J. Akers, Gail P. Sudlow, Siavash Yazdanfar, Samuel Achilefu, "Quantitative determination of maximal imaging depth in all-NIR multiphoton microscopy images of thick tissues," Proc. SPIE 8948, Multiphoton Microscopy in the Biomedical Sciences XIV, 894827 (28 February 2014); doi: 10.1117/12.2036868

SPIE.

Event: SPIE BiOS, 2014, San Francisco, California, United States

Quantitative determination of maximal imaging depth in all-NIR multiphoton microscopy images of thick tissues

Pinaki Sarder[a], Walter J. Akers[a], Gail P. Sudlow[a], Siavash Yazdanfar[b], Samuel Achilefu[a*]

[a]Department of Radiology, Washington University School of Medicine, CB 8225, 4225 Scott Av., St. Louis, MO 63108, USA;
[b]Applied Optics Laboratory, GE Global Research, Niskayuna, NY 12309, USA

*Correspondence: achilefus@mir.wustl.edu

ABSTRACT

We report two methods for quantitatively determining maximal imaging depth from thick tissue images captured using all–near-infrared (NIR) multiphoton microscopy (MPM). All-NIR MPM is performed using 1550 nm laser excitation with NIR detection. This method enables imaging more than five-fold deep in thick tissues in comparison with other NIR excitation microscopy methods. In this study, we show a correlation between the multiphoton signal along the depth of tissue samples and the shape of the corresponding empirical probability density function (pdf) of the photon counts. Histograms from this analysis become increasingly symmetric with the imaging depth. This distribution transitions toward the background distribution at higher imaging depths. Inspired by these observations, we propose two independent methods based on which one can automatically determine maximal imaging depth in the all-NIR MPM images of thick tissues. At this point, the signal strength is expected to be weak and similar to the background. The first method suggests the maximal imaging depth corresponds to the deepest image plane where the ratio between the mean and median of the empirical photon-count pdf is outside the vicinity of 1. The second method suggests the maximal imaging depth corresponds to the deepest image plane where the squared distance between the empirical photon-count mean obtained from the object and the mean obtained from the background is greater than a threshold. We demonstrate the application of these methods in all-NIR MPM images of mouse kidney tissues to study maximal depth penetration in such tissues.

Keywords: Near-infrared (NIR), cyanine dyes, all-NIR multiphoton microscopy.

1. INTRODUCTION

The development of multi-photon microscopy (MPM) has stimulated advances in thick tissue imaging[1, 2]. MPM employs pulsed near-infrared (NIR) laser sources with the width of pulses in the femto-second duration to excite target fluorecent molecules. During this process, the respective fluorophore molecules absorb two simultaneous NIR photons, each of which carries slightly more than half of the energy than that required for single-photon excitation. This requirement for simultaneous absorption of two photons means the probability of excitation is greatest at the focal point illumination, thus reducing photobleaching and eliminating out-of-focus fluorescence and the need for pinholes used in conventional confocal fluorescence microscopy imaging. This also results in a significantly greater effective Stokes shift, eliminating crosstalk between excitation and emission detection. MPM achieves greater axial resolution (0.4 μm) in imaging, and penetrates hundreds of microns deeper into tissues due to the NIR excitation[3, 4].

While researchers have been exploiting the power of MPM in performing deep tissue fluorescence microscopy, focus on using the unique advantages of NIR wavelengths (>700 nm) for this purpose has gained interest in the last ten years[5]. Namely, fluorescence imaging at visible wavelengths is limited due to high auto-fluorescence and light scattering. These issues become severe for low target concentrations, necessitating the use of strategies that reduce auto-fluorescence and improve the signal-to-noise ratio (SNR). Researchers have addressed these problems by leaning more toward performing fluorescence imaging at NIR wavelengths to minimize auto-fluorescence and increase light penetration of tissue. Along

Multiphoton Microscopy in the Biomedical Sciences XIV, edited by Ammasi Periasamy, Peter T. C. So, Karsten König, Proc. of SPIE Vol. 8948, 894827 · © 2014 SPIE
CCC code: 1605-7422/14/$18 · doi: 10.1117/12.2036868

this direction, we developed a new all-NIR MPM[6-8]. This imaging method uses femto-second wide pulses at ~1550 nm wavelength[6], and it is able of imaging molecules that fluoresce at NIR wavelengths.

In a recent study using intact kidney tissues containing NIR cyanine contrast agents, we have demonstrated all-NIR MPM imaging method can image more than five-fold (>500 μm) deeper than existing single- and two-photon NIR excitation microscopy methods[7]. Using all-NIR MPM, we also showed that multiphoton signal along tissue depth correlates with the shape of the corresponding empirical probability density function (pdf) of the photon counts. We have observed such histograms become increasingly symmetric with the imaging depth. Our study shows that the histograms approach the background distribution as we image deeper into the tissues. Inspired by these observations, we suggest two methods based on which maximal imaging depth can be quantitatively determined from all-NIR MPM images of thick tissues. Signal strength from such imaging depth is expected to be weak and similar to the background.

2. MATERIALS AND METHODS

2.1 Contrast agents

To perform the imaging experiment, we used LS288 contrast agent. This dye was synthesized as described previously[9]. Detailed optical properties of this contrast agent are available in our earlier publication[7].

2.2 Ex vivo kidney samples preparation

We performed the animal studies in compliance with the Washington University School of Medicine (WUSM) Animal Studies Committee requirements for the humane care and use of laboratory animals in research. For the study described herein, we used samples of highly scattering murine kidney tissue samples for imaging. To prepare the samples, we anesthetized ten-week-old male FVB/N mice with isoflurane (2% v/v) in 100% oxygen via precision vaporizer, and sacrificed those mice 30 s after intravenous injection of 60 μM Cy3 or LS288 dissolved in 100 μL PBS. This process ensured a significant accumulation of dye molecules in the mouse kidneys. Immediately after euthanasia, the kidneys were harvested intact and rinsed with PBS and subsequently imaged using the all-NIR MPM method.

2.3 All–near-infrared multi-photon microscopy

All-NIR MPM was performed using a custom-built system as previously reported[6]. This system consists of a mode-locked fiber laser (Mercury 1550-200-150-INS, PolarOnyx, San Jose, CA), a galvanometric mirror pair (6215H, Cambridge Technology, Lexington, MA), a dichroic mirror (LP02-980RS, Semrock, Rochester, New York), a 20×, 0.95-NA water-immersion objective lens (XLUMPLFLN 20XW, Olympus), a thermoelectrically cooled, red-enhanced GaAs PMT and photon counting head (H7421-50, Hamamatsu), and a multifunction data acquisition card (DAQ) (PCI-6229, National Instruments, Austin, TX). The laser provides excitation light centered near ~1575 nm through a 0.75 m single-mode fiber patch cord. The cord output provides transform-limited pulses of nominal durations 100 fs with frequency 43.7 MHz and of average power 170 mW. The laser is optimized by the vendors to deliver transform-limited pulses out of a 1 m optical fiber, but the fiber was shortened to partially pre-compensate for material dispersion in the system described here. The PMT operates in photon-counting mode at 380-890 nm, with peak sensitivity at 800 nm.

To obtain the all-NIR MPM fluorescence images, laser light was collimated, expanded by a factor of 5, and directed through the dichroic mirror and objective lens onto the sample. The objective collected two-photon epifluorescence from the sample and directed it towards the PMT using the dichroic mirror. A 3 mm thick glass filter (RG9, Schott, Elmsford, NY) removed the residual excitation light. The DAQ measured the 5 V digital output pulses from the PMT. We acquired the images by raster scanning the target FOV in the sample with the excitation beam using the galvanometric mirror pair. Custom-built Labview software controlled the image acquisition and instrument. We compute the spatial resolution of this state-of-the-art MPM to be 0.6 μm. A detailed discussion on this instrument, including point-spread function measurements and confirmation of square law relationship between signal and incident power, is available in our earlier publication[6].

2.4 Deep tissue fluorescence microscopy imaging

Prior to microscopy, a whole-kidney sample was gently covered with a cover-glass of thickness 0.17 mm. During the imaging, the sample was exposed to 5.55 mW of laser power with 1 ms/pixel. To obtain such power in the sample, a continuously variable neutral density (ND) filter (NDC-50C-2, Thorlabs, Newton, NJ) was adjusted during the imaging. The laser power was adjusted to be 30 mW below the objective, which was effectively 5.55 mW below the water immersion media before the cover-glass, due to the heavy water absorption of light at 1575 nm[7]. Image stacks of FOV

172.2 μm × 172.2 μm with 25.4 μm steps were captured during the imaging, with spatial sampling interval as 0.67 μm. A background image was also obtained by scanning the imaging stage with the laser light in the absence of the kidney sample.

2.5 Statistical analysis

To analyze the shape of the empirical pdf of the photon counts, histograms of such counts from the image planes are generated using MATLAB with number of bins as 20. To depict the symmetry of the shapes of such pdfs, Gaussian curves are fitted with them with means as the histogram peaks and variances same as the histogram variances. Ratio between the histogram mean and median is computed for each image plane, and compared with a threshold bound along the image depth of focus inside the kidney sample. Mean square distance between the mean of the photon count histogram from each image plane and the mean of the histogram obtained from the background image is also computed, and the resulting distance is compared with a threshold along the image depth of focus inside the kidney sample.

3. RESULTS AND DISCUSSION

3.1 All-near-infrared multiphoton microscopy extended depth resolution[7]

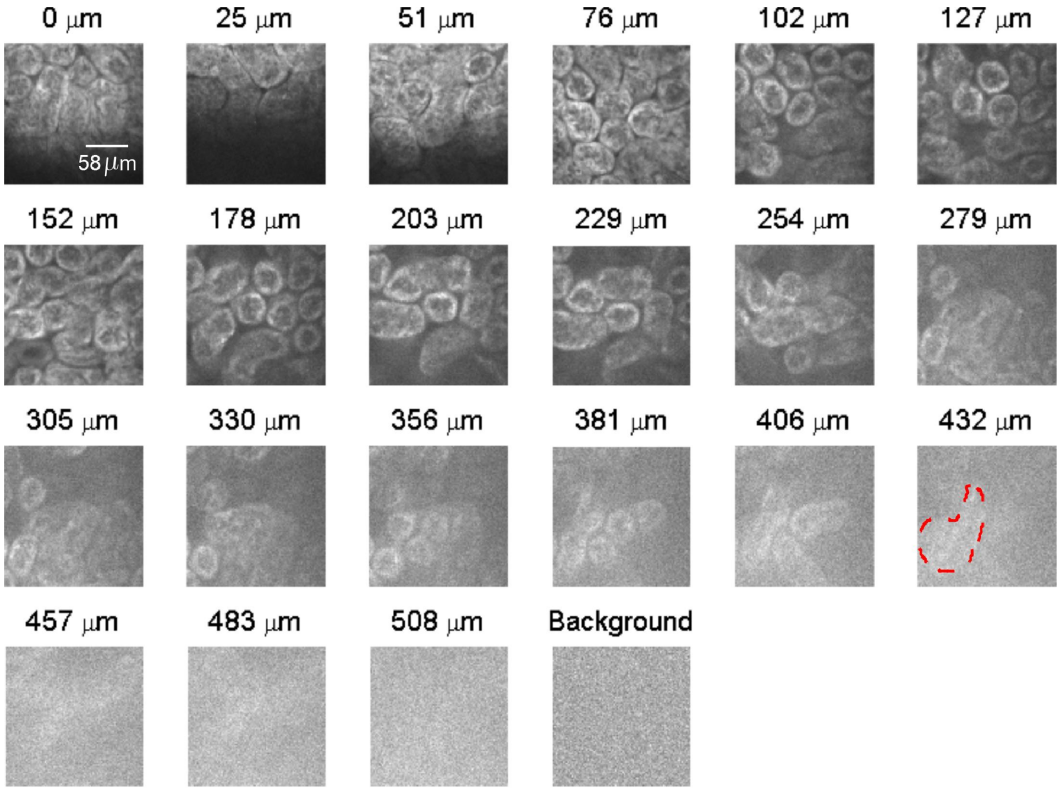

Figure 1. All-NIR MPM image stack of mouse kidney *ex vivo*. The mouse kidney was harvested after intravenous injection of NIR dye LS288. The structure of renal tubules in the kidney cortex can be visualized down to >400 μm below the specimen surface. Dashed red line indicates the structure visible in a noisy background at 432 μm imaging depth.

Using the all-NIR MPM system to image intact kidney sample from mouse containing LS288, the fluorescence contrast was detected from the surface down to >400 μm (Fig. 1). Renal tubules were visualized in the resulting images. The result confirms our previous finding on the depth penetration capability of the all-NIR MPM system. This result also reflects the combined benefits of lower scattering and absorption of the NIR light used for both dye excitation and emission, as well as the selective focal plane illumination of the two-photon imaging mechanism.

3.2 Empirical probability density function of photon counts becomes symmetric along the depth in deep tissue imaging using all–near-infrared multiphoton microscopy

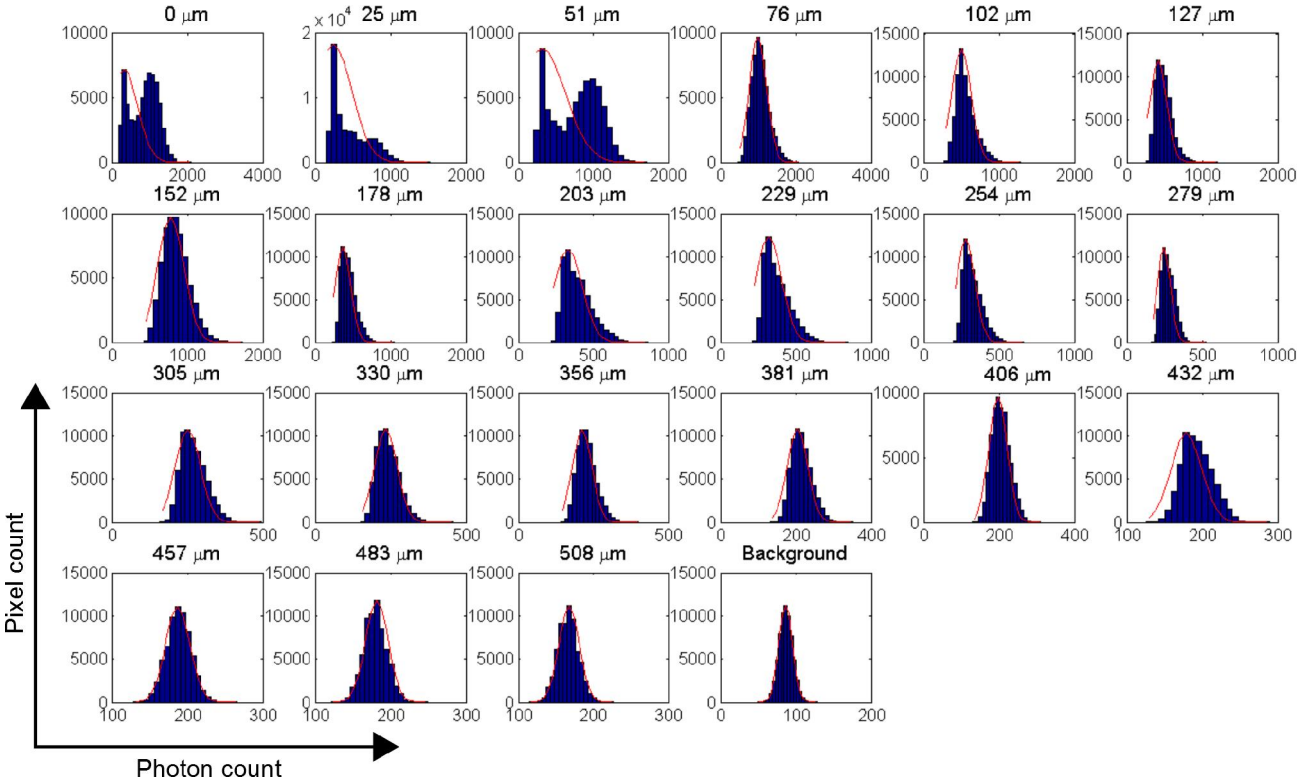

Figure 2. Empirical pdfs of photon counts along the depth during imaging mouse kidney using the all-NIR MPM system. Gaussian curve is fitted with each of the empirical pdfs to depict the symmetry or asymmetry associated with the pdf shapes. The shape of the empirical pdfs becomes symmetric as we image deeper inside the tissue.

The empirical pdfs of the photon counts along the depth are shown in Fig. 2. We observe the shape of the pdf becomes increasingly symmetric as we image deeper in kidney tissue. Such shapes in the initial imaging planes show two modes in the respective distributions, which is probably because the kidney structures do not fill completely the FOV of imaging in such planes. The next few planes resemble asymmetric pdf, and depict Poisson distribution which indeed models photon counts. For the images obtained from the deeper planes (>432 μm), the pdf shape becomes increasingly symmetric where the signal strength from the structures are increasingly weaker from one plane to the next adjacent plane. These symmetric distributions resemble Gaussian distribution. Similar distribution is also observed for the background. This result demonstrates that the signal strength along the depth during all-NIR MPM imaging correlates with the shape of the empirical pdfs of the corresponding photon counts.

3.3 Method 1: Maximal imaging depth corresponds to the deepest image plane into the tissue, where the ratio between the mean and median of the empirical photon-count pdf is outside the vicinity of 1

Based on the above findings, we postulate that the shape information of the empirical pdf of photon counts during deep tissue imaging using all-NIR MPM can provide a method for automatically determining the maximal imaging depth. For symmetric pdfs, the ratio of their mean and median converges to 1. Similarly, the skewness of these pdfs converges to 0. We confine studying the ratio between the mean and median of each of such pdfs along the imaging depth. This ratio is plotted for the kidney tissue images shown in Fig. 1 as a function of the imaging depth. We hypothesize that when this metric falls within an interval specified by 0.95 and 1.05, the structures in the corresponding deep tissue images become invisible or indistinguishable from the background. For the images shown in Fig. 1, this point occurred at imaging depths >406 μm. In addition, Fig. 1 indicates that the images captured beyond this depth are indeed noisy. Therefore, the ratio between the mean and median of the empirical pdf is potentially a useful metric for automatically determining maximal imaging depth in tissues imaged using all-NIR MPM imaging. Based on this method, the maximal imaging depth in a

tissue imaged by the all-NIR MPM system corresponds to the deepest image plane where this ratio metric is outside the interval of 0.95 to 1.05.

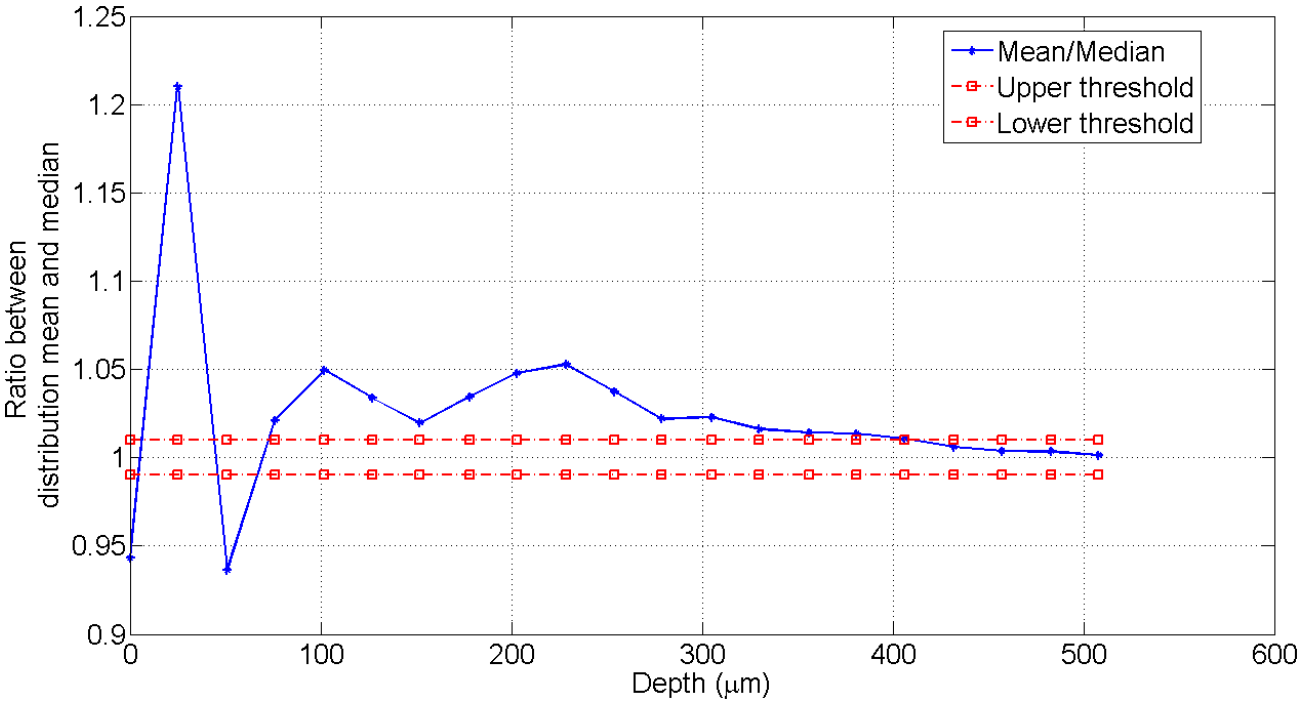

Figure 3. Ratio between the mean and median of the empirical pdf of photon counts along the depth during imaging mouse kidney using the all-NIR MPM system. The ratio converges to 1 with increasing depth. We suggest the maximal imaging depth corresponds to the deepest image plane where such ratio is outside of an interval specified at the vicinity of 1.

3.4 Method 2: Maximal imaging depth corresponds to the deepest image plane into the tissue where the squared distance between the empirical photon-count mean obtained from the imaging object and such mean obtained from the background is greater than a threshold

As discussed in Section 3.2, the squared distance between the mean of the empirical pdf of photon counts from an imaging plane of a thick tissue sample and the mean of the empirical pdf of photon counts from background is a useful metric for automatically determining the maximal imaging depth in thick tissues imaged using the all-NIR MPM system. This metric is studied as a function of imaging depth in Fig. 4 for the kidney images shown in Fig. 1. The squared distance decreases with the imaging depth, after depicting a zigzag pattern in the initial imaging planes. The data suggest that the maximal imaging depth corresponds to the distance metric, where such metric is below 10^4. The corresponding images captured using the all-NIR MPM system are noisy, and the structures in these images are indistinguishable from the background. Based on this method, the maximal imaging depth in the above example is 457 μm, which is close to the maximal depth based on the criterion suggested in Section 3.3. The threshold is chosen to be 10^4, as we experimentally found about 100 more photon counts per pixel due to the near-surface fluorescence when the kidney sample is very close to the objective during imaging[10]. The laser provided by the vendor also has a tail in its spectrum which bleeds-through the detector, resulting in a higher photon count than expected during the near-surface fluorescence measurement.

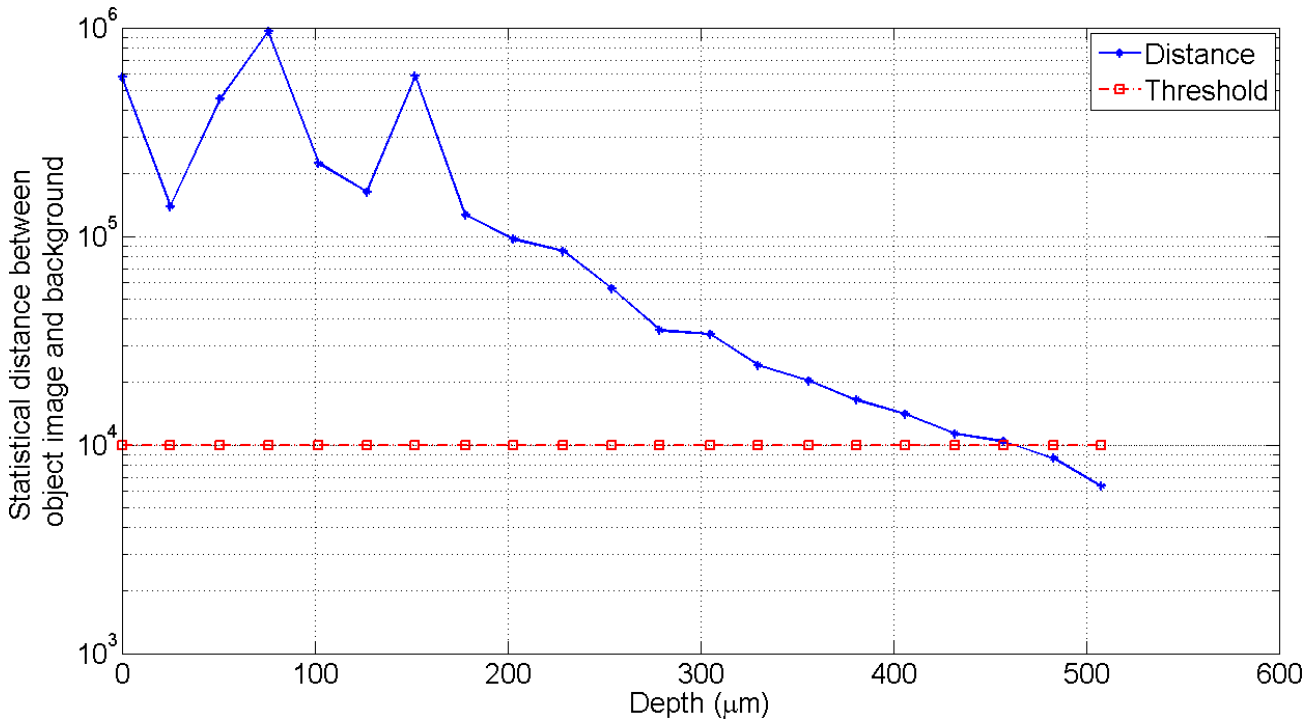

Figure 4. Squared distance between the means of the empirical pdfs of the photon counts generated from mouse kidney and from background during imaging using the all-NIR MPM system as a function of imaging depth. This distance metric decreases after depicting an initial zigzag pattern. We suggest maximal imaging depth as the deepest image plane, where this metric falls below a predefined threshold.

4. CONCLUSION

In this paper, we have extended our earlier study on deep tissue imaging using all-NIR MPM system[7], and suggested methods that can be used for automatically determining maximal imaging depth from deep tissues imaged using the all-NIR MPM system. The first method suggests the maximal imaging depth as the deepest plane in the tissue where the ratio between the mean and median of the empirical photon-count pdf is outside an interval defined in the vicinity of 1. The second method suggests the maximal imaging depth as the deepest plane where the squared distance between the empirical photon-count mean obtained from the object and such mean obtained from the background is greater than a threshold. The proposed methods are formed from our observation in several kidney tissue samples, and a representative example is used for the presentation provided above. In a future study, we will extend this work for deep tissue imaging using other fluorescence microscopy methods, as well as for diverse organs of mice containing fluorescent molecular probes.

5. ACKNOWLEDGMENT

This study was supported by grants from the National Institutes of Health (NCI R21/R33 CA123537 and NIBIB R01 EB008111).

6. REFERENCES

[1] Denk, W., Strickler, J. H. and Webb, W. W., "Two-photon laser scanning fluorescence microscopy," Science, 248(4951), 73-6 (1990).

[2] Zipfel, W. R., Williams, R. M. and Webb, W. W., "Nonlinear magic: multiphoton microscopy in the biosciences," Nature Biotechnology, 21(11), 1369-77 (2003).

[3] Theer, P., Hasan, M. T. and Denk, W., "Two-photon imaging to a depth of 1000 microm in living brains by use of a Ti:Al2O3 regenerative amplifier," Optics Letters, 28(12), 1022-4 (2003).

[4] Squirrell, J. M., Wokosin, D. L., White, J. G. *et al.*, "Long-term two-photon fluorescence imaging of mammalian embryos without compromising viability," Nature Biotechnology, 17(8), 763-7 (1999).

[5] Achilefu, S., "The insatiable quest for near-infrared fluorescent probes for molecular imaging," Angewandte Chemie, 49(51), 9816-8 (2010).

[6] Yazdanfar, S., Joo, C., Zhan, C. *et al.*, "Multiphoton microscopy with near infrared contrast agents," Journal of biomedical optics, 15(3), 030505 (2010).

[7] Sarder, P., Yazdanfar, S., Akers, W. J. *et al.*, "All-near-infrared multiphoton microscopy interrogates intact tissues at deeper imaging depths than conventional single- and two-photon near-infrared excitation microscopes," Journal of Biomedical Optics, 18(10), 106012 (2013).

[8] Berezin, M. Y., Zhan, C., Lee, H. *et al.*, "Two-photon optical properties of near-infrared dyes at 1.55 mum excitation," The journal of physical chemistry. B, 115(39), 11530-5 (2011).

[9] Lee, H., Mason, J. C. and Achilefu, S., "Heptamethine cyanine dyes with a robust C-C bond at the central position of the chromophore," The Journal of organic chemistry, 71(20), 7862-5 (2006).

[10] Theer, P. and Denk, W., "On the fundamental imaging-depth limit in two-photon microscopy," J Opt Soc Am A Opt Image Sci Vis, 23(12), 3139-49 (2006).